



# CHORUS

This is the accepted manuscript made available via CHORUS. The article has been published as:

## Effect of Growth Induced (Non)Stoichiometry on Interfacial Conductance in $\text{LaAlO}_3/\text{SrTiO}_3$

E. Breckenfeld, N. Bronn, J. Karthik, A. R. Damodaran, S. Lee, N. Mason, and L. W. Martin

Phys. Rev. Lett. **110**, 196804 — Published 9 May 2013

DOI: [10.1103/PhysRevLett.110.196804](https://doi.org/10.1103/PhysRevLett.110.196804)

# Effect of Growth-Induced (Non)Stoichiometry on Interfacial Conductance of $\text{LaAlO}_3/\text{SrTiO}_3$

E. Breckenfeld<sup>1</sup>, N. Bronn<sup>2</sup>, J. Karthik<sup>1</sup>, A. R. Damodaran<sup>1</sup>, S. Lee<sup>1</sup>, N. Mason<sup>2</sup>, and L. W. Martin<sup>1\*</sup>

<sup>1</sup>*Department of Materials Science and Engineering and Materials Research Laboratory,  
University of Illinois, Urbana-Champaign, Urbana, IL 61801 and*

<sup>2</sup>*Department of Physics and Materials Research Laboratory,  
University of Illinois, Urbana-Champaign, Urbana, IL 61801*

(Dated: April 1, 2013)

We demonstrate a link between the growth process, the stoichiometry of  $\text{LaAlO}_3$ , and the interfacial electrical properties of  $\text{LaAlO}_3/\text{SrTiO}_3$  heterointerfaces. Varying the relative La:Al cation stoichiometry by a few atomic percent in films grown at  $1 \times 10^{-3}$  Torr results in a two and seven order-of-magnitude change in the 300K and 2K sheet resistance, respectively, with highly conducting states occurring only in La-deficient or Al-excess films. Further reducing the growth pressure results in an increase of the carrier density and a dramatic change in mobility. We discuss the relative contributions of intrinsic and extrinsic effects in controlling the physical properties of this widely studied system.

Since the discovery of a conducting state at the  $\text{LaAlO}_3/\text{SrTiO}_3$  heterointerface in 2004[1], researchers have uncovered a series of other exciting phenomena[2–6]. The conductivity is hypothesized to arise from electronic reconstruction that occurs to avoid the so-called polar catastrophe[1]. This reconstruction occurs at a critical thickness of just  $<4$  unit cells[7–9] and can be considered an intrinsic response of the system to the build-up of electrostatic energy. Structural distortions[10–13] and chemical intermixing,[14–16] which are expected to occur since ionic crystals terminated at oppositely charged polar surfaces are inherently unstable and can undergo surface reconstructions/intermixing to maintain electrostatic stability (e.g., Ge/GaAs),[17, 18] have additionally been considered as potential responses. Recent work has highlighted such imperfection in  $\text{LaAlO}_3/\text{SrTiO}_3$ [19] and probed the evolution of the polar catastrophe with chemical alloying[20]. Extrinsic effects, in particular oxygen vacancies, have also been observed to play a role in the conductivity of these samples[2, 21]. Varying the growth pressure of oxygen results in dramatic changes in the interfacial conductivity[2], with growth at low pressures ( $<1 \times 10^{-5}$  Torr) resulting in high carrier mobility ( $>10^4$   $\text{cm}^2/\text{V-s}$ ) and three-dimensional transport, while growths at higher pressures result in a transition to non-metallic behavior (suggesting the potential role of oxygen vacancies in the substrate as a likely source of the observed transport)[21]. Ultimately understanding and utilizing these intrinsic and extrinsic effects is an important challenge.

The murkiness of our understanding may, in part, be related to the complexity associated with the synthesis of these heterointerfaces. Such variations in the pulsed-laser deposition (PLD) growth process can have a profound impact on the subsequent heterostructure properties. It is difficult to obtain stoichiometric  $\text{LaAlO}_3$  films via PLD[15, 22] and researchers have observed as much as 11% La-excess in films grown in conditions consistent with those used for work on conducting heterointerfaces[22]. Studies focusing on the relationship between laser fluence and film stoichiometry for perovskites[23–26] indicate that synthesizing films with nearly perfect stoichiometry may be the exception, not

the default result for PLD. This could explain the fact that although many have observed conducting interfaces, there are wide variations in carrier concentration, mobility, and temperature dependence as a result of slight variations in the growth conditions. It is likely that multiple factors are active in this system, providing for a complex interplay of intrinsic/extrinsic effects and muddled property evolution.

With this in mind, we investigate the direct relationship between variations in  $\text{LaAlO}_3$  cation stoichiometry and properties of the  $\text{LaAlO}_3/\text{SrTiO}_3$  heterointerface. We study the evolution of sheet resistance, carrier concentration, and mobility of the  $\text{LaAlO}_3/\text{SrTiO}_3$  heterointerfaces as a function of both cation and oxygen stoichiometry. We observe that variation in the La:Al cation stoichiometry of several atomic percent results in a two and seven order-of-magnitude change in the 300K and 2K sheet resistance, respectively, with highly conducting states occurring only in La-deficient or Al-excess films. Further, reducing the growth pressure results in an increase in the sheet carrier density and a dramatic change in the carrier mobility.

10 unit cell thick  $\text{LaAlO}_3$  films were grown via reflection high-energy electron diffraction (RHEED)-assisted PLD at  $750^\circ\text{C}$ . A frequency of 1 Hz was used for the growth of all samples and the growth rate for all films was 12 pulses/unit cell. Films were grown from a single crystal  $\text{LaAlO}_3$  target (Crystec, GmbH) on  $\text{TiO}_2$ -terminated  $\text{SrTiO}_3$  (001) substrates treated via standard methods[27, 28]. Growths were completed at a range of pressures and oxidizing potentials and throughout the manuscript we will directly identify the growth pressure of each film studied. All samples were cooled at  $10^\circ\text{C}/\text{min}$  at growth pressure. For samples grown at  $1 \times 10^{-3}$  Torr the laser fluence was varied between 1.2 and 2.0  $\text{J}/\text{cm}^2$  by changing the laser spot size from 0.043  $\text{cm}^2$  to 0.071  $\text{cm}^2$  while holding the incident laser energy constant (85 mJ). Note that these energy densities are within ranges previously reported[1, 2, 22, 26, 29]. In order to maintain the appropriate stoichiometry, slight adjustments of the laser fluence were required at other pressures. All growths were completed with the laser focused on the target in an imaging mode (Supplemental Materials, Table. S1)[30].

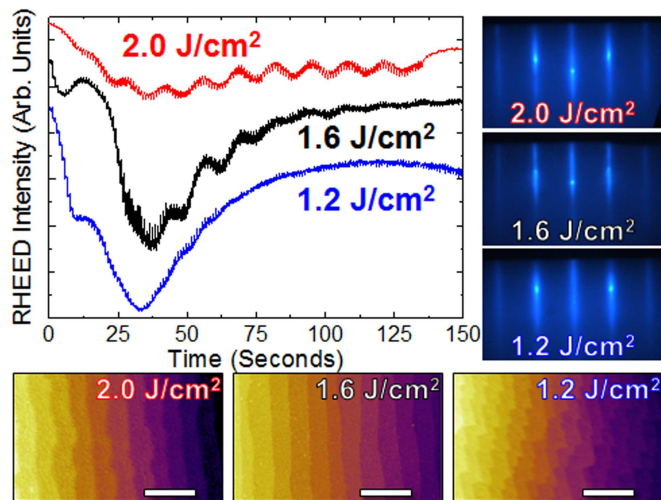


FIG. 1: RHEED oscillations as well as post-growth RHEED images (right) and AFM images (bottom) of films grown at laser fluences of 1.2 (blue), 1.6 (black), and 2.0 (red)  $\text{J}/\text{cm}^2$ .

Growths were completed in an on-axis geometry with a target-substrate distance of 6.6 cm. All interfacial transport measurements were completed on 10 unit cell (3.79 nm) thick  $\text{LaAlO}_3$  films and additional films up to 200 nm were grown for structural and compositional analysis.

*In situ* RHEED studies were used to track the evolution of growth modes and establish growth rates for all depositions [Fig 1]. Typical time-dependent RHEED intensity profiles for 10 unit cell thick films grown at 1.2, 1.6, and 2.0  $\text{J}/\text{cm}^2$  reveal an evolution from step-flow or hybrid-growth to layer-by-layer growth with increasing laser fluence. Typical post-growth RHEED patterns [right, Fig 1] and *ex situ* atomic force microscopy (AFM) [bottom, Fig 1] reveal evidence of smooth, atomic-level terraced, island-free films in all cases. While the growth mode varied somewhat with laser fluence, there are no other indications in the RHEED or AFM to suggest significant differences in the films. Thus at these growth conditions ( $1 \times 10^{-3}$  Torr and  $750^\circ\text{C}$ ), although smooth films are achieved at various fluence values, the generally sought after layer-by-layer growth regime is only achieved at higher fluence (2.0  $\text{J}/\text{cm}^2$ ). Subsequent x-ray diffraction studies reveal that all films are single-phase and epitaxial (for clarity we show data from 60 nm thick films [Fig. 2(a)], but results for 10 unit cell (3.79 nm) and 200 nm  $\text{LaAlO}_3/\text{SrTiO}_3$  (001) heterostructures are also provided, Supplemental Materials [Fig. S1])[30]. We observed a slight expansion of the out-of-plane lattice parameter of the  $\text{LaAlO}_3$  films with increasing laser fluence [Fig. 2(a), inset], consistent with prior studies, and [26, 31], based on reciprocal space mapping studies [Supplemental Materials Fig. S2][30], the films are found to be partially or nearly completely relaxed.

X-ray photoelectron spectroscopy (XPS) and Rutherford backscattering spectrometry (RBS) were used to further investigate the effect of laser fluence on the cation stoichiometry. Prior work showed a strong relationship between stoichiometry and deposition angle in  $\text{LaAlO}_3$  [15, 22, 31] and this work provides complimentary studies of the role laser fluence. The XPS studies focused

on the La 3d and Al 2p peaks [Supplemental Materials, Fig. S3(a),(b), respectively][30], as these peaks account for the dominant contribution to the XPS signal for their respective elements. Additional details of the XPS measurements and the calibration are provided [Supplemental Materials [Fig. S3(c),(d)][30]. RBS studies were completed to confirm the XPS results and verify that the film composition is the same throughout the thickness [Supplemental Materials, Fig. S4]. The XPS and RBS studies are considered to have  $\pm 1\%$  and  $\pm 0.75\%$  error bars, respectively. Both the trends and overall compositional values found from the XPS and RBS studies were consistent and show a strong relationship between PLD laser fluence and film stoichiometry [Fig. 2(b)].

Focusing first on films grown at  $1 \times 10^{-3}$  Torr (100%  $\text{O}_2$ ), films grown at a fluence of 1.6  $\text{J}/\text{cm}^2$  were observed to exhibit an average chemical formula of  $\text{La}_{1.01}\text{Al}_{0.99}\text{O}_{3-x}$  (corresponding to a  $[\text{La}]/([\text{La}]+[\text{Al}])$  ratio of 50.5%) and are henceforth referred to as *stoichiometric* films. Increasing the fluence to 2.0  $\text{J}/\text{cm}^2$  yields films with an average chemical formula of  $\text{La}_{0.92}\text{Al}_{1.08}\text{O}_{3-x}$  (corresponding to a  $[\text{La}]/([\text{La}]+[\text{Al}])$  ratio of 46%) and are henceforth referred to as *La-deficient* (or Al-excess) films. Finally, decreasing the fluence to 1.2  $\text{J}/\text{cm}^2$  yields films with an average chemical formula of  $\text{La}_{1.12}\text{Al}_{0.88}\text{O}_{3-x}$  (corresponding to a  $[\text{La}]/([\text{La}]+[\text{Al}])$  ratio of 56%) and are henceforth referred to as *La-excess* (or Al-deficient) films. These trends in non-stoichiometry are consistent with recent studies [32] which suggest that higher laser fluence will preferentially ablate Al from the  $\text{LaAlO}_3$  target leading to a deficiency of La in the film while lower laser fluence ablates the target more evenly but results in Al deficiencies in the film since the lighter Al adatoms scatter more readily in the growth gas. Additionally, we have studied the effect of growth pressure on the film composition and have found it to have a less dramatic effect. Changing the pressure from  $1 \times 10^{-3}$  to  $1 \times 10^{-6}$  Torr, the slope of the compositional variation with laser fluence decreases, but the overall trend remains the same (i.e., 4-5% La-deficiency is achieved at  $1 \times 10^{-6}$  Torr at 2.2  $\text{J}/\text{cm}^2$ ).

To reiterate, there is little indication from the *in situ* RHEED, the *ex situ* AFM, and the x-ray diffraction studies that would have indicated such a large deviation in the stoichiometry of the  $\text{LaAlO}_3$  films. Thus, in addition to the fact that it can be difficult to obtain stoichiometric films, it is also difficult to detect deviations in stoichiometry using standard methods. The lack of observed second phases additionally indicates that the (non)stoichiometry, in all cases, is either within the effective solubility limit for La-deficiency and -excess for  $\text{LaAlO}_3$  or that the fractions of any secondary phases are below the sensitivity of the diffraction experiments and do not manifest visibly on the surface. From these experiments, it appears that in this deposition geometry, the laser fluence is the dominant parameter responsible for controlling film stoichiometry. Armed with this knowledge, we further investigated the effect of film stoichiometry on the electrical properties of the heterointerface.

The interfacial electrical properties of 10 unit cell thick

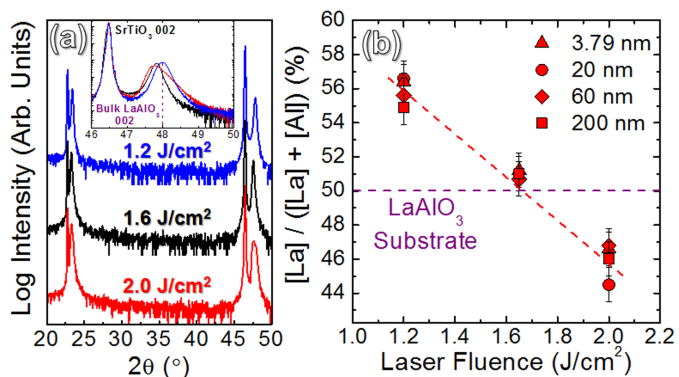


FIG. 2: (a) Wide angle and (inset) zoom-in x-ray diffraction scan for 60nm LaAlO<sub>3</sub>/SrTiO<sub>3</sub> (001) heterostructures grown at various laser fluences. (b) Cation atomic ratio as a function of fluence in numerous LaAlO<sub>3</sub> films as measured by XPS.

LaAlO<sub>3</sub> films were probed using temperature and field-dependent resistivity studies (details in Supplemental Materials)[30]. We focus first on films grown at  $1 \times 10^{-3}$  Torr (100% O<sub>2</sub>). Stoichiometric films exhibit metallic-like conductivity from room temperature down to 38K, where they experience a crossover from metallic-like to weakly insulator-like conduction (henceforth referred to as a crossover transition) [black curve, Fig 3(a)]. Note that the sheet resistance of the stoichiometric film is relatively flat, varying only one order-of-magnitude from 2-300K. La-excess films likewise exhibit metallic-like conductivity from room temperature down to 55K, where they also undergo a crossover transition and a large increase in sheet resistance down to 2K [blue curve, Fig. 3(a)]. We also note other anomalies in the data for both the La-excess and stoichiometric films, particularly kinks near 70-80 and 155-180K which have been observed previously[33, 34] and have been attributed to surface structural transitions in SrTiO<sub>3</sub>[35, 36]. Finally, La-deficient films exhibit metallic-like conductivity from room temperature to 10K, where they exhibit a slight increase in resistance down to 2K [wine, red curves, Fig. 3(a)]. To further illustrate the effect of stoichiometry on the properties, we have included films with 2% and 4% La-deficiency and we see that there is an inverse relationship between the 2K sheet resistance and the extent of La-deficiency. In all cases, La-deficient films possess low-temperature sheet resistances that are at least 1-3 orders-of-magnitude lower than that of the stoichiometric films and 5-7 orders-of-magnitude lower than that of the La-excess films.

There are a number of important points to make in summarizing these findings. First, using the growth process (in particular laser fluence) to manipulate and control the cation (non)stoichiometry, we have recreated sheet resistance trends which have been previously attributed purely to oxygen pressure variations, and consequently, to oxygen vacancies[2, 21, 33, 37]. Second, there is a clear change in the crossover transition temperature with La-cation stoichiometry with more La-deficiency leading to suppressed crossover transition temperatures suggesting a potential change in the nature of the interfacial conductance. Third, as a clarification of the first point, La-deficient films grown at  $1 \times 10^{-3}$  Torr reveal

metallic-like conductivity typical of films generally grown at much lower oxygen pressures (note that many consider this pressure to be above that which would allow for interfacial conductance). We believe that this could potentially be correlated to a cation (non)stoichiometry driven reduction of the substrate. While oxygen vacancies likely have a role to play in the behavior of the heterointerface, the cation stoichiometry of the LaAlO<sub>3</sub> film could also affect the electrical behavior in these heterostructures.

A number of recent studies support this hypothesis. First-principles calculations[38] have shown that LaAlO<sub>3</sub>/SrTiO<sub>3</sub> heterointerfaces with La-deficiency (or Al-excess) have higher densities of La- and O-vacancy Schottky pairs and these oxygen vacancies are generally quite mobile and are known to cluster in the SrTiO<sub>3</sub> substrate under even mildly reducing conditions[39, 40]. Additionally, a recent experiment suggests that a metallic state can be induced on the surface of SrTiO<sub>3</sub> crystals by deposition of oxygen deficient alumina (Al<sub>2</sub>O<sub>3-x</sub>), granular aluminum films, or spinel  $\gamma$ -Al<sub>2</sub>O<sub>3</sub> films, which effectively reduce the SrTiO<sub>3</sub> leading to an oxygen vacancy induced conducting state[41, 42]. Such observations are supported by investigation of Ellingham diagrams which reveal that Al possesses a large free energy of oxidation (the Al curve lies well below the Ti curve on the diagram) and thus in an oxygen starved environment, Al can be expected to reduce the SrTiO<sub>3</sub>.

In turn, we have also investigated the effect of varying the growth pressure on the electrical properties. We focus here on 4% La-deficient films and investigate a number of different oxidation conditions:  $1 \times 10^{-3}$  Torr (100% O<sub>2</sub> and 0.01% O<sub>3</sub>-99.99% O<sub>2</sub>) and  $1 \times 10^{-6}$  Torr (100% O<sub>2</sub> and 10% O<sub>3</sub>-90% O<sub>2</sub>). In all cases XPS and RBS studies have been completed to assure consistent composition. The subsequent temperature dependent resistivity studies reveal the ability to fine tune the nature of conductance with oxygen stoichiometry. La-deficient films grown in more reducing conditions display similar trends in their sheet resistance (metallic-like conductivity to low temperatures), with more reducing growth conditions resulting in diminished sheet resistance [Fig. 3(a)]. We also note that growth of both La-deficient and stoichiometric films at  $1 \times 10^{-3}$  Torr in 0.01% O<sub>3</sub> 99.99% O<sub>2</sub> had essentially no effect on the observed resistivity compared to the growth in 100% O<sub>2</sub> at the same pressure, and that post-growth anneals in oxygen had little impact on the conductivity in these samples. More importantly, however, the films grown at  $1 \times 10^{-6}$  Torr (regardless of ozone inclusion) reveal no clear crossover to insulator-like behavior down to 2K. This is not expected for true two-dimensional systems which should exhibit localization of electrons[43] and an up-turn in resistivity at low temperatures[44]. Instead, it is consistent with prior studies which have shown a transformation from two- to three-dimensional conduction in films grown at low pressures[21]. This transformation in dimensionality of the conductivity is further supported by the fact that clear indications of the SrTiO<sub>3</sub> surface structural transitions[33-36] are no longer visible in the electrical transport studies of the La-deficient films (a strong indicator that the conduction is no longer localized to the



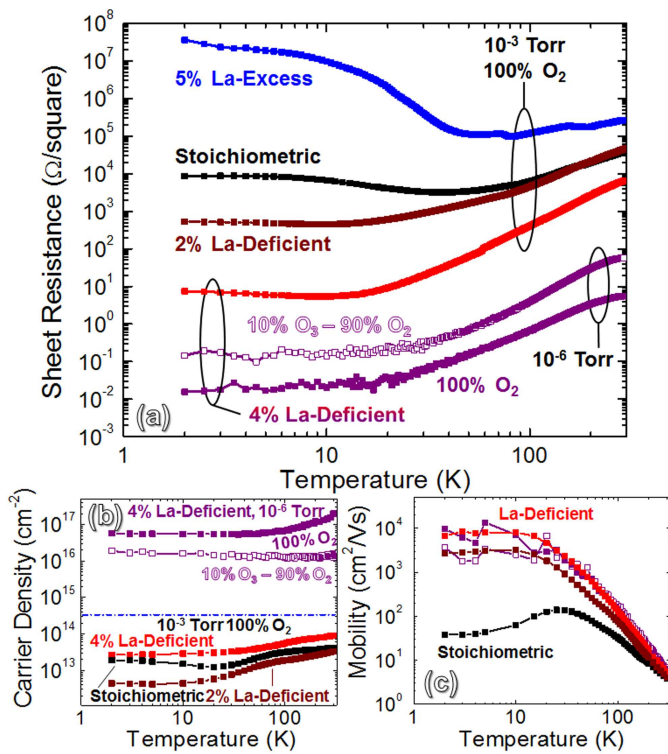


FIG. 3: (a) Sheet resistance as a function of temperature for 10 unit cell thick La-excess, stoichiometric, and La-deficient films grown at a variety of oxygen and ozone pressures. (b) Sheet carrier density and (c) carrier mobility for the same films.

film-substrate interface).

We have also probed the sheet carrier density [Fig. 3(b)] and mobility [Fig. 3(c)] as a function of temperature. No data for the carrier concentration or mobility is provided for the La-excess films, as the sheet resistance was too high to obtain reliable results. The theoretical sheet carrier density expected from electronic reconstruction to alleviate the polar catastrophe is half an electron per unit cell or  $3.3 \times 10^{14} \text{ cm}^{-2}$  (which serves as an effective theoretical maximum value of possible carriers [dashed line, Fig. 3(b)]). The carrier concentration for both the stoichiometric and La-deficient films grown at  $1 \times 10^{-3}$  Torr are all at least one order-of-magnitude smaller than this theoretical value. The films grown at a pressure of  $1 \times 10^{-6}$  Torr, however, reveal sheet carrier densities between  $10^{16}$ - $10^{18} \text{ cm}^{-2}$ , unrealistic values well in excess of the theoretical value [Fig. 3(b)]. This is consistent with prior studies[1, 21] and with the concept that the conduction must be spilling over into the bulk of the SrTiO<sub>3</sub>. Similarly, there are two distinct types of carrier mobility [Fig. 3(c)]. At all temperatures studied, the carrier mobility of the stoichiometric film is found to be less than the carrier mobility for the La-deficient films. Furthermore, the stoichiometric films reveal a maximum carrier mobility at 38K (corresponding to the crossover transition) before decreasing to 2K. On the other hand, all La-deficient films display very similar mobility trends, increasing with decreasing temperature and then essentially plateauing around  $10^3$ - $10^4 \text{ cm}^2/\text{V-s}$  below 25K, consistent with values reported in high-quality SrTiO<sub>3</sub> films[45].

To summarize, the conduction in the case of the La-

excess and stoichiometric films is consistent with what is expected for a two-dimensional interfacial state arising from intrinsic effects such as electronic reconstruction to avoid the polar-catastrophe (in the absence of an obviously dominating extrinsic explanation). This is supported by the fact that the overall sheet resistance is higher, that the carrier density values are lower than the theoretical maximum, that clear indications of surface reconstructions in SrTiO<sub>3</sub> are observed, and that the carrier mobility is lower. For the case of the La-deficient films, growth at  $1 \times 10^{-3}$  Torr results in metallic-like conductance which is attributed to the cation (non)stoichiometry which could potentially drive reduction of the SrTiO<sub>3</sub> and subsequent substrate contributions to conductance. Finally, in films grown at  $1 \times 10^{-6}$  Torr, extremely low sheet resistance, the complete suppression of the crossover transition, the extraordinarily high sheet carrier densities, and the large carrier mobility are consistent with the onset of significant substrate reduction and substrate-based conductivity.

In turn, it appears that cation stoichiometry can be an essential parameter that must be understood and controlled to access the intrinsic physics of the LaAlO<sub>3</sub>/SrTiO<sub>3</sub> heterointerface. By controlling the film stoichiometry to within 5% of the ideal value, we observed dramatic variations in conductance, as intrinsic and extrinsic contributions to the interfacial conductance compete. Such insights may be instrumental in further study of the physical phenomena at these interfaces.

The authors would like to acknowledge Rick Haasch and Doug Jeffers at the Center for Microanalysis of Materials at UIUC. Work on the control and characterization of stoichiometry in pulsed-laser deposition grown films was supported by the U.S. Department of Energy under grant DEFG02-07ER46459. Work on the study of electronic transport was supported by the National Science Foundation and the Nanoelectronics Research Initiative under grant DMR-1124696. Experiments at UIUC were carried out in part in the Materials Research Laboratory Central Facilities.

\* Electronic address: [lwmartin@illinois.edu](mailto:lwmartin@illinois.edu)

- [1] A. Ohtomo, H. Y. Hwang, *Nature* **427**, 423 (2004).
- [2] A. Brinkman, M. Huijben, M. van Zalk, J. Huijben, U. Zeitler, J. C. Maan, W. G. van der Wiel, G. Rijnders, D. H. A. Blank, H. Hilgenkamp, *Nature Mater.* **6**, 493 (2007).
- [3] N. Reyren, S. Thiel, A. D. Caviglia, L. Fitting-Kourkoutis, G. Hammerl, C. Richter, C. W. Schneider, T. Kopp, A.S. Retschi, D. Jaccard, M. Gabay, D. A. Muller, J. M. Triscone, J. Mannhart, *Science* **317**, 1196 (2007).
- [4] G. Singh-Bhalla, C. Bell, J. Ravichandran, W. Siemons, Y. Hikita, S. Salahuddin, A. F. Hebard, H. Y. Hwang, R. Ramesh, *Nature Phys.* **7**, 80 (2011).
- [5] J. W. Park, D. F. Bogorin, C. Cen, D. A. Felker, Y. Zhang, C. T. Nelson, C. W. Bark, C. M. Folkman, X. Q. Pan, M. S. Rzchowski, J. Levy, C. B. Eom, *Nature Commun.* **1**, 94 (2010).
- [6] C. Cen, S. Thiel, G. Hammerl, C. W. Schneider, K. E. Andersen, C. S. Hellberg, J. Mannhart, J. Levy, *Nature Mater.* **7**, 298 (2008).

- [7] S. Thiel, G. Hammerl, A. Schmehl, C. W. Schneider, J. Mannhart, *Science* **313**, 1942 (2006).
- [8] C. Bell, S. Harashima, Y. Hikita, H. Y. Hwang, *Appl. Phys. Lett.* **94**, 222111 (2009).
- [9] M. Breitschaft, V. Tinkl, N. Pavlenko, S. Paetel, C. Richter, J. R. Kirtley, Y. C. Liao, G. Hammerl, V. Eyert, T. Kopp, J. Mannhart, *Phys. Rev. B* **81**, 153414 (2010).
- [10] J. L. Maurice, C. Carrtro, M. J. Casanove, K. Bouzehouane, S. Guyard, J. Larquet, J.P. Contour, *Phys. Stat. Sol. a* **203**, 2209 (2006).
- [11] R. Pentcheva, W. E. Pickett, *Phys. Rev. Lett.* **102**, 107602 (2009).
- [12] J. Verbeeck, S. Bals, A. N. Kravtsova, D. Lamoen, M. Luysberg, M. Huijben, G. Rijnders, A. Brinkman, H. Hilgenkamp, D. H. A. Blank, G. Van Tendeloo, *Phys. Rev. B* **81**, 085113 (2010).
- [13] J. E. Boschker, C. Folkman, C. W. Bark, A. F. Monsen, E. Folven, J. K. Grepstad, E. Wahlström, C. B. Eom, T. Tybell, *Phys. Rev. B* **84**, 205418 (2011).
- [14] P. R. Willmott, S. A. Pauli, C. M. Schlepztz, D. Martoccia, B. D. Patterson, B. Delley, R. Clarke, D. Kumah, C. Cionca, Y. Yacoby, *Phys. Rev. Lett.* **99**, 155502 (2007).
- [15] L. Qiao, T. C. Droubay, V. Shutthanandan, Z. Zhu, P. V. Sushko, S. A. Chambers, *J. Phys.: Condens. Matter* **22**, 312201 (2010).
- [16] A. S. Kalabukhov, Y. A. Boikov, I. T. Serenkov, V. I. Sakharov, V. N. Popok, R. Gunnarsson, J. Brjesson, N. Ljustina, E. Olsson, D. Winkler, T. Claeson, *Phys. Rev. Lett.* **103**, 146101 (2009).
- [17] G. A. Baraff, J. A. Appelbaum, D. R. Hamann, *Phys. Rev. Lett.* **38**, 237 (1977).
- [18] W. A. Harrison, E. A. Kraut, J. R. Waldrop, R. W. Grant, *Phys. Rev. B* **18**, 4402 (1978).
- [19] S. A. Chambers, M. H. Engelhard, V. Shutthanandan, Z. Zhu, T. C. Droubay, L. Qiao, P. V. Sushko, T. Feng, H. D. Lee, T. Gustafsson, E. Garfunkel, A. B. Shah, J.M. Zuo, Q. M. Ramasse, *Surf. Sci. Rep.* **65**, 317 (2010).
- [20] M. L. Reinle-Schmitt, C. Cancellieri, D. Li, D. Fontaine, M. Medarde, E. Pomjakushina, C. W. Schneider, S. Gariglio, P. Ghosez, J.-M. Triscone, P. R. Willmott, *Nature Commun.* **3**, 932 (2012).
- [21] G. Herranz, M. Basleti, M. Bibes, C. Carrtro, E. Tafra, E. Jacquet, K. Bouzehouane, C. Deranlot, A. Hamzi, J.-M. Broto, A. Barthlmy, A. Fert, *Phys. Rev. Lett.* **98**, 216803 (2012).
- [22] T. C. Droubay, L. Qiao, T. C. Kaspar, M. H. Engelhard, V. Shutthanandan, S. A. Chambers, *Appl. Phys. Lett.* **97**, 124105 (2010).
- [23] T. Ohnishi, M. Lippmaa, T. Yamamoto, S. Meguro, H. Koinuma, *Appl. Phys. Lett.* **87**, 241919 (2005).
- [24] T. Ohnishi, K. Shibuya, T. Yamamoto, M. Lippmaa, *Appl. Phys. Lett.* **103**, 103703 (2008).
- [25] E. Breckenfeld, R. Wilson, J. Karthik, A. R. Damodaran, D. G. Cahill, L. W. Martin, *Chem. Mater.* **242**, 331 (2012).
- [26] F. Schoofs, T. Fix, A.S. Kalabukhov, D. Winkler, Y. Boikov, I. Serenkov, V. Sakharov, T. Claeson, J.L. MacManus-Driscoll, M.G. Blamire, *J. Phys.: Condens. Matter* **23**, 305002 (2011).
- [27] M. Kawasaki, K. Takahashi, T. Maeda, R. Tsuchiya, M. Shinohara, O. Ishiyama, T. Yonezawa, M. H. Yoshimoto, Koinuma, *Science* **266**, 1540 (1994).
- [28] T. Ohnishi, K. Shibuya, M. Lippmaa, D. Kobayashi, H. Kumigashira, M. Oshima, *Appl. Phys. Lett.* **85**, 272 (2004).
- [29] A. Koitzsch, J. Ocker, M. Knupfer, M.C. Dekker, K. Dorr, B. Buchner, P. Hoffmann, *Phys. Rev. B* **84**, 245121 (2011).
- [30] See Supplemental Material at <http://link.aps.org/supplemental/10.1103/PhysRevLett.000.000000> for a detailed description the laser fluence and spot size determination, additional x-ray diffraction studies, raw XPS spectral data for the various samples, and RBS spectra and analysis.
- [31] L. Qiao, T.C. Droubay, T. Varga, M. E. Bowden, V. Shutthanandan, Z. Zhu, T. C. Kaspar, S. A. Chambers, *Phys. Rev. B* **83**, 085408 (2011).
- [32] S. Wicklein, A. Sambri, S. Amoruso, X. Wang, R. Bruzzese, *Appl. Phys. Lett.* **101**, 131601 (2012).
- [33] W. Siemons, G. Koster, H. Yamamoto, T. H. Geballe, D. H. A. Blank, M. R. Beasley, *Phys. Rev. B* **76**, 155111 (2007).
- [34] F. Schoofs, M. Egilmez, T. Fix, J. L. MacManus-Driscoll, M. G Blamire, *Appl. Phys. Lett.* **100**, 081601 (2012).
- [35] Z. Salman, R. F. Kiefl, K. H. Chow, M. D. Hossain, T. A. Keeler, S. R. Kreitzman, C. D. P. Levy, R. I. Miller, T. J. Parolin, M. R. Pearson, H. Saadaoui, J. D. Schultz, M. Smadella, D. Wang, W. A. MacFarlane, *Phys. Rev. Lett.* **96**, 147601 (2006).
- [36] Z. Salman, M. Smadella, W. A. MacFarlane, B. D. Patterson, P. R. Willmott, K. H. Chow, M. D. Hossain, H. Saadaoui, D. Wang, R. F. Kiefl, *Phys. Rev. B* **83I**, 224112 (2011).
- [37] A. Kalabukhov, R. Gunnarsson, J. Brjesson, E. Olsson, T. Claeson, D. Winkler, *Phys. Rev. B* **75**, 121404R (2007).
- [38] X. Luo, B. Wang, Y. Zheng, *Phys. Rev. B* **80**, 104115 (2009).
- [39] Z. Zhong, P. X. Xu, P. J. Kelly, *Phys. Rev. B* **82**, 165127 (2010).
- [40] G. L. Yuan, L. W. Martin, R. Ramesh, A. Uedono, *Appl. Phys. Lett.* **95**, 012904 (2009).
- [41] J. Delahaye, T. Grenet, *J. Phys. D Appl. Phys.* **45**, 315301 (2012).
- [42] Y. Z. Chen, N. Bovet, F. Trier, D. V. Christensen, F. M. Qu, N. H. Andersen, T. Kasama, W. Zhang, R. Giraud, J. Dufouleur, T. S. Jespersen, J. R. Sun, A. Smith, J. Nygard, L. Lu, B. Buchner, B. G. Shen, S. Linderoth, N. Pryds, *Nature Comm.* **4**, 1371 (2013).
- [43] E. Abrahams, S. V. Kravchenko, M. P. Sarachik, *Rev. Mod. Phys.* **73**, 251 (2001).
- [44] E. Abrahams, P. W. Anderson, D. C. Licciardello, T. V. Ramakrishnan, *Phys. Rev. Lett.* **42**, 673 (1979).
- [45] J. Son, P. Moetakef, B. Jalan, O. Bierwagen, N. J. Wright, R. Engel-Herbert, S. Stemmer, *Nature Mater.* **9**, 482 (2010).